SRTTU

JCARME

ISSN: 2228-7922

Journal of Computational and Applied Research in Mechanical Engineering
Vol. x, No. x, xxxx
jcarme.sru.ac.ir

Dynamic response of a shaft of a Pelton turbine due to impact of water jet

Mahesh Chandra Luintel[a,*] and Tri Ratna Bajracharya[a]

[a] *Department of Mechanical Engineering, Pulchowk Campus, Institute of Engineering, Tribhuvan University 44700, Nepal*

Abstract

Performance and reliability of any rotating machine can be studied by proper dynamic analysis of the machine. In this regard, this paper presents the method to study the dynamic response of the shaft of a Pelton turbine due to the impact of water jet. Equations of motion for the bending vibration of Pelton turbine assembly, in two transverse directions, is developed by using Lagrange equation of motion with the help of assumed modes method. The Pelton wheel is assumed as a rigid disk attached on an Euler-Bernoulli shaft. The impact provided by the water jet is represented in the form of Fourier series. Critical speeds of the system are determined by performing free vibration analysis and presented in the form of Campbell diagram. The response plots due to impact of water are generated by performing forced response analysis. Both free and forced analyses are carried out by considering first three modes of vibration.

Nomenclature

Ω	Spin speed of shaft, rad/s
ρ	Density of material of shaft, kg/m^3
ρ_d	Density of material of disk, kg/m^3
ω	Angular velocity, rad/s
A	Cross sectional area of the shaft, m^2
C_i	Modal damping
E	Modulus of Elasticity, Pa
$F(t)$	Force exerted on the disk
h	Thickness of the disk, m
$\mathbf{i}, \mathbf{j}, \mathbf{k}$	Unit vectors along x, y and z axes respectively
I_d	Second moment of area of disk section, m^4
I_s	Second moment of area of shaft section, m^4
J_{pd}	Polar second moment of area of disk section, m^4
J_{ps}	Polar second moment of area of shaft section, m^4
K_i	Modal stiffness
L	Length of the shaft, m
M_d	Mass of disk, kg
M_i	Modal mass
$\mathbf{r_s}$	Position vector of any point of shaft
T	Kinetic energy
U_s	Strain energy of the shaft
v	Displacement along y axis
$V(t)$	Dynamic amplitude of transverse vibration in horizontal direction
v_s	Velocity vector of any point of the shaft
w	displacement along z axis
$W(t)$	Dynamic amplitude of transverse vibration in vertical direction
W_{ext}	External work
x	Direction along longitudinal axis of the shaft

[*] *Corresponding author*
Email address: mcluintel@ioe.edu.np

y Transverse horizontal direction of the shaft
z Transverse vertical direction of the shaft.

Keywords:

Pelton Turbine, Flexible shaft, Free response, Forced response, Impact of jet

1. Introduction

Most of the power producing and power consuming units consist of a disk attached to a shaft. One of the most common examples of this is a Pelton turbine unit used for electricity generation in hydropower plants. Pelton turbines are high head turbines used for both small and large power generation. These rotating turbines are subjected to highly hostile working conditions. The design and manufacturing challenge is concerned with improvement in performance, life and reduction in weight without loss of reliability. There are numerous possibilities of excitation by external disturbances and the behaviour of the system under those disturbance can be predicted to some extent by the appropriate dynamic analysis.

The dynamic response of such shaft-disk system depends upon many components and operating parameters. Different researchers have investigated different aspects of a rotodynamic system by modelling the system as an assembly of a rigid disk attached to an Euler-Bernoulli shaft. Sabuncu *et al.* [1] have investigated the critical speed of a rotor consisting of a single disc on a solid shaft by treating the shaft as a rotating beam element using transfer matrix-finite element model. Rajalingham *et al.* [2] have investigated the influence of external damping on rotor response to imbalance of gravity excitations and have shown that sufficient amount of damping can suppress the reported instability caused by anisotropic bending stiffness characteristics. Lee *et al.* [3] have analyzed the effect of the direction of application and magnitude of loads on the stability and natural frequency of flexible rotors subjected to non-conservative torque and force.

Khader [4] has investigated the stability of the rotating cantilever shaft with a rigid disk at its free end subjected to periodic follower axial force and end moment. Silva *et al.* [5] have studied the bending vibration of a machine rotor by using the Euler-Bernoulli beam theory, as a continuous beam, subjected to a specific set of boundary conditions. Chattoraj *et al.* [6] have considered a two dimensional isotropic and flexible horizontal rotor with a symmetrical disk including the effects of gravity and coriolis forces. Gundogdu *et al.* [7] have presented simulations of a continuous cantilever beam and an unbalanced disk system by extending classical Jeffcott rotor approach to a model that gives the first three (or more) modes of the flexible beam.

Shahgholi *et al.* [8] have also investigated the two rotor systems, one of which has been comprised of a symmetrical shaft and an asymmetrical disk, and the other one has been comprised of an asymmetrical shaft and an asymmetrical disk. Lin *et al.* [9] has used finite element simulation to develop several models of single-rotor system, with different numbers of shaft elements, relative number of degrees of freedom and, by using, four types of modelling for the shaft and disk interface. Han [10] has performed complex harmonic analysis for rotor based upon Floquet theory and has presented the modal features of each critical speed both by quantitatively and qualitatively.

Huang [11] has studied the characteristics of torsional vibration of a rotor with unbalance by numerical simulation.

Some researchers have studied non-linear phenomena in shaft-disk systems. Chang *et al.* [12] have analyzed instability and non-linear dynamics of a simply supported slender shaft made of a viscoelastic material and have determined stability. Genta *et al.* [13] have extended the usual mathematical models based on the finite element method to the study of the dynamic behaviour of rotors with non-constant angular speed by considering both the nonlinear behaviour of the rotor and its geometrical or inertial anisotropy. Inoue *et al.* [14] have investigated the chaotic vibration due to the 1 to

(−1) type internal resonance at the major critical speed and twice the major critical speed. Diken *et al.* [15] have considered a Jeffcott rotor and have derived the non-linear dynamic equations of the rotor and shown that there exists two subharmonic transient vibrations caused by the non-linearity of the system itself. Shad *et al.* [16] have investigated the nonlinear dynamics of rotors by developing a mathematical model incorporating the higher order deformations in bending, rotary inertia, gyroscopic effect, rotor mass unbalance and dynamic axial force. Phadatare *et al.* [17] have formulated strongly coupled non-linear equations of motion, based on strain energy and kinetic energy equations for shaft, disk and unbalance mass, with shaft undergoing large bending deformations to determine the nonlinear frequencies and resultant dynamic behaviour of high speed rotor bearing system with mass unbalance.
Similarly, some researchers have investigated the coupled bending and torsional vibration of the shaft disk systems. Al-Bedoor [18] has developed a model for coupled torsional and lateral vibrations of an unbalanced rotor and has shown through simulation that there exists an energetic interaction between the rotor torsional and lateral vibration. Xiang *et al.* [19] have studied the vibration characteristics on flexural and torsional modes of a Jeffcott rotor system with rigid support. Alnefaie *et al.* [20] have considered a rotating flexible shaft-disk system to study the torsional vibration coupled with the lateral and longitudinal vibration, and have shown that, while the shaft speed changes, torsional natural frequency of the shaft-disk system and longitudinal natural frequency of the beam does not change but lateral natural frequency of the beam changes.
Another area dealt by many researchers is the dynamic response of the rotodynamic system due to different kind of interactions on the disk of the system. Kojima *et al.* [21] have investigated the torsional vibrations of a rotating shaft system having a disk and a magnet coupling in which the driver of the magnet coupling is excited by sinusoidal motion and the disk is subjected to constant load torque.
Few research works have been carried out to study the effect of looseness on the behavior of the shaft-disk system. Muszynska *et al.* [22] have presented the results of numerical simulation of the dynamic behavior of a one-lateral-mode rotor, which is unbalanced and radially side-loaded, with either a loose pedestal (looseness in a stationary joint), or with occasional rotor-to-stator rubbing in which the nonlinearities are associated with the rotor intermittent contacts with the stationary element. Behzad et al. [23] have used energy method to calculate rotor response with loose rotating disk on it and shown that the clearance between loose disk and shaft, shaft speed, mass and mass moment of inertia of disk have a major effect on a rotor response and beating phenomena.
Many researchers have extensively studied the effect of rub impact on dynamic behavior of the shaft-disk system. Azeez *et al.* [24] have worked to obtain the transient response of an overhung rotor undergoing vibro-impacts due to a defective bearing with reference to an overhung rotor clamped on one end, with a flywheel on the other and impacts occurring in between, due to a bearing with clearance. Shen *et al.* [25] have investigated the vibration characteristics of a rub-impact rotor-bearing system excited by mass unbalance including mass eccentricity and initial permanent deflection. Jian *et al.* [26] have studied the nonlinear dynamic analysis of the rotor–bearing system supported by oil-film short bearings, with nonlinear suspension, by considering the rub–impact between rotor and stator for precise analysis of rotor-bearing systems. Khanlo *et al.* [27] have studied the chaotic vibration analysis of a rotating flexible continuous shaft-disk system with rub impact. Khanlo *et al.* [28] have also investigated the lateral–torsional coupling effects on the nonlinear dynamic behavior of a rotating flexible shaft–disk system. Jiao *et al.* [29] have developed a dynamic model to study the characteristics of unbalanced rotor system with external excitations including the influences of gyroscopic effect, gravity and static/dynamic unbalance. Ma *et al.* [30] have investigated the nonlinear dynamic characteristics of a single span rotor system

with two discs under fixed-point and local arc rub-impact conditions. Tai *et al.* [31] have investigated the stability and steady-state response of the rotor system using a lumped mass model of a single rub-impact rotor system considering the gyroscopic effect.

Wahab *et al.* [32] have studied the parametric instability behaviour for a simple shaft and disk system subjected to axial load under pinned-pinned boundary condition and have found that the additional disk mass decreases the instability region during static condition and the location of the disk also has significant effect on the instability region of the shaft. Chen *et al.* [33] have developed a model based on finite element method and Lagrange's equation to study the dynamic behavior of flexible rotor system subjected to time-variable base motions and have found that the base rotations would cause nonlinearities.

Most of the earlier papers have focused the dynamic response of a flexible shaft due to intervention from the surroundings such as rub impact or effects of bearing properties. This paper focus mainly on the dynamic response of the shaft-disk system to impact of general tangential forces on the disk which can used to study the behavior of a Pelton turbine subjected to impact of water jet.

2. Problem Formulation

2.1 System Kinematics and Energy Expressions for the System

Consider a rigid disk attached to a flexible shaft as shown in Fig. 1. The axes *x*, *y* and *z* are chosen such that *x* is along longitudinal direction of the shaft, y is along transverse direction of shaft on the horizontal plane and *z* is along the transverse direction of the shaft on the vertical plane. Similarly, transverse displacements of any point of the shaft along horizontal and vertical directions are respectively $v(x,t)$ and $w(x,t)$. For the horizontal shaft, Pelton turbine water jet acts along the *y* direction.

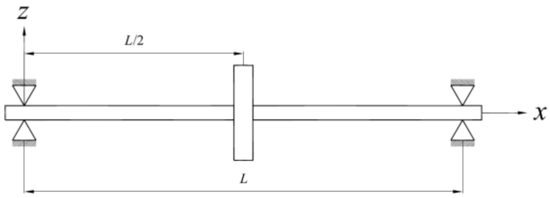

Fig. 1. Shaft-disk assembly

The velocity of any point on neutral axis of the shaft with reference to inertial frame is given by [27]

$$\boldsymbol{v_s} = (\dot{v} - \Omega w)\boldsymbol{j} + (\dot{w} + \Omega v)\boldsymbol{k} \qquad (1)$$

The angular velocity vector of the shaft element is given by [27]

$$\boldsymbol{\omega_e} = (\Omega + v'\dot{w}')\boldsymbol{i} + (-\Omega v' - \dot{w}')\boldsymbol{j} + (-\Omega w' + \dot{v}')\boldsymbol{k} \qquad (2)$$

Then kinetic energy of the shaft is given by

$$T = \frac{1}{2}\rho A\int_0^L [(\dot{v} - \Omega w)^2 + (\dot{w} + \Omega v)^2]dx + \frac{1}{2}\rho J_{ps}\int_0^L [(\Omega + v'\dot{w}')^2]\,dx + \frac{1}{2}\rho I_s\int_0^L [(-\Omega v' - \dot{w}')^2 + (-\Omega w' + \dot{v}')^2]\,dx \qquad (4)$$

Avoiding higher order terms, kinetic energy of the shaft given by Eq. (3) can be expressed as

$$T_s = \frac{1}{2}\rho A\int_0^L \dot{v}^2 dx + \frac{1}{2}\rho A\int_0^L \dot{w}^2 dx + \frac{1}{2}\rho A\Omega^2\int_0^L v^2 dx + \frac{1}{2}\rho A\Omega^2\int_0^L w^2 dx + \rho A\Omega\int_0^L \dot{w}v dx - \rho A\Omega\int_0^L \dot{v}w dx + \frac{1}{2}\rho J_{ps}\Omega^2 L + \rho J_{ps}\Omega\int_0^L \dot{w}'v'\,dx + \frac{1}{2}\rho I_s\int_0^L \dot{v}'^2 dx + \frac{1}{2}\rho I_s\int_0^L \dot{w}'^2 dx + \frac{1}{2}\rho I_s\Omega^2\int_0^L v'^2 dx + \frac{1}{2}\rho I_s\Omega^2\int_0^L w'^2 dx + \rho I_s\Omega\int_0^L \dot{w}'v'\,dx - \rho I_s\Omega\int_0^L \dot{v}'w'\,dx \quad (4)$$

Similarly, kinetic energy of the disk can be expressed as

$$T_d = \frac{1}{2}M_d(\dot{v}^2)\Big|_{x=\frac{L}{2}} + \frac{1}{2}M_d(\dot{w}^2)\Big|_{x=\frac{L}{2}} + \frac{1}{2}M_d\Omega^2(v^2)\Big|_{x=\frac{L}{2}} + \frac{1}{2}M_d\Omega^2(w^2)\Big|_{x=\frac{L}{2}} + M_d\Omega(\dot{w}v)\Big|_{x=\frac{L}{2}} - M_d\Omega(\dot{v}w)\Big|_{x=\frac{L}{2}} + \frac{1}{2}\rho_d hJ_{pd}\Omega^2 + \rho_d hJ_{pd}\Omega(\dot{w}'v')\Big|_{x=\frac{L}{2}} + \frac{1}{2}\rho_d hI_d\left(\dot{v}'^2\right)\Big|_{x=\frac{L}{2}} + \frac{1}{2}\rho_d hI_d\left(\dot{w}'^2\right)\Big|_{x=\frac{L}{2}} + \frac{1}{2}\rho_d hI_d\Omega^2\left(v'^2\right)\Big|_{x=\frac{L}{2}} + \frac{1}{2}\rho_d hI_d\Omega^2\left(w'^2\right)\Big|_{x=\frac{L}{2}} + \rho_d hI_d\Omega(\dot{w}'v')\Big|_{x=\frac{L}{2}} - \rho_d hI_d\Omega(\dot{v}'w')\Big|_{x=\frac{L}{2}} \quad (5)$$

The strain energy of the shaft due to bending is then given by

$$U_s = \frac{1}{2}EI_s\int_0^L [(v'')^2 + (w'')^2]dx \quad (6)$$

Work done by the impact of jet is given by

$$W_{ext} = F(t)(v)\Big|_{x=\frac{L}{2}} \quad (7)$$

2.2 Equation of Motion for the System

For assumed mode method, displacement variables can be assumed as

$$v = \{\phi(x)\}^T\{V(t)\} = \{\phi\}^T\{V\} \quad (8)$$

$$w = \{\phi(x)\}^T\{W(t)\} = \{\phi\}^T\{W\} \quad (9)$$

Substituting v and w into Eqs. (4) to (7) and using Lagrange equation

$$\frac{d}{dt}\left(\frac{\partial T}{\partial \dot{q}}\right) - \frac{\partial T}{\partial q} + \frac{\partial U}{\partial q} - \frac{\partial W_{ext}}{\partial q} = 0 \quad (10)$$

we get equations of motion for transverse vibrations as

$$\rho A\int_0^L[\{\phi\}\{\phi\}^T\{\ddot{V}\}]dx + \rho I_s\int_0^L[\{\phi'\}\{\phi'\}^T\{\ddot{V}\}]dx + M_d[\{\phi\}_d\{\phi\}_d{}^T\{\ddot{V}\}] + \rho_d hI_d[\{\phi'\}_d\{\phi'\}_d{}^T\{\ddot{V}\}] - 2\rho A\Omega\int_0^L[\{\phi\}\{\phi\}^T\{\dot{W}\}]dx - 2\rho I_s\Omega\int_0^L[\{\phi'\}\{\phi'\}^T\{\dot{W}\}]\,dx - 2M_d\Omega[\{\phi\}_d\{\phi\}_d{}^T\{\dot{W}\}] - 2\rho_d hI_d\Omega[\{\phi'\}_d\{\phi'\}_d{}^T\{\dot{W}\}] - \rho J_{ps}\Omega\int_0^L[\{\phi'\}\{\phi'\}^T\{\dot{W}\}]\,dx - \rho_d hJ_{pd}\Omega[\{\phi'\}_d\{\phi'\}_d{}^T\{\dot{W}\}] - \rho A\Omega^2\int_0^L[\{\phi\}\{\phi\}^T\{V\}]dx - \rho I_s\Omega^2\int_0^L[\{\phi'\}\{\phi'\}^T\{V\}]dx - M_d\Omega^2[\{\phi\}_d\{\phi\}_d{}^T\{V\}] - \rho_d hI_d\Omega^2[\{\phi'\}_d\{\phi'\}_d{}^T\{V\}] + EI_s\int_0^L[\{\phi''\}\{\phi''\}^T\{V\}]dx - F(t)\{\phi\}_d = \{0\} \quad (11)$$

$$\rho A\int_0^L[\{\phi\}\{\phi\}^T\{\ddot{W}\}]dx + \rho I_s\int_0^L[\{\phi'\}\{\phi'\}^T\{\ddot{W}\}]dx + M_d[\{\phi\}_d\{\phi\}_d{}^T\{\ddot{W}\}] + \rho_d hI_d[\{\phi'\}_d\{\phi'\}_d{}^T\{\ddot{W}\}] + 2\rho A\Omega\int_0^L[\{\phi\}\{\phi\}^T\{\dot{V}\}]dx + \rho J_{ps}\Omega\int_0^L[\{\phi'\}\{\phi'\}^T\{\dot{V}\}]\,dx + 2\rho I_s\Omega\int_0^L[\{\phi'\}\{\phi'\}^T\{\dot{V}\}]\,dx + 2M_d\Omega[\{\phi\}_d\{\phi\}_d{}^T\{\dot{V}\}] + \rho_d hJ_{pd}\Omega[\{\phi'\}_d\{\phi'\}_d{}^T\{\dot{V}\}] + 2\rho_d hI_d\Omega[\{\phi'\}_d\{\phi'\}_d{}^T\{\dot{V}\}] - \rho A\Omega^2\int_0^L[\{\phi\}\{\phi\}^T\{W\}]dx - \rho I_s\Omega^2\int_0^L[\{\phi'\}\{\phi'\}^T\{W\}]dx - M_d\Omega^2[\{\phi\}_d\{\phi\}_d{}^T\{W\}] - \rho_d hI_d\Omega^2[\{\phi'\}_d\{\phi'\}_d{}^T\{W\}] + EI_s\int_0^L[\{\phi''\}\{\phi''\}^T\{W\}]dx = \{0\} \quad (12)$$

3. Response of the System

3.1 Discretization of Equation of Motion

For the assumed mode method, we can assume

$$\phi_i = sin\left(\frac{i\pi x}{L}\right) \quad (13)$$

which are the eigenfunctions of a simply supported non-rotating beam.

Substituting $\{\phi\} = \{\phi_1 \quad \phi_2 \quad .... \quad \phi_n\}^T$ into Eqs. (11) and (12), we get a system of linear ordinary differential equations for each assumed mode as

$$M_i\ddot{V}_i(t) - C_i\dot{W}_i(t) + K_iV_i(t) = F_i(t) \quad (14)$$

$$M_i\ddot{W}_i(t) + C_i\dot{V}_i(t) + K_iW_i(t) = 0 \quad (15)$$

where

$$M_i = \frac{1}{2}\rho AL + \frac{\pi^2 i^2}{2L}\rho I_s + M_d\, sin^2\left(\frac{i\pi}{2}\right) + \frac{\pi^2 i^2}{L^2}\rho_d h I_d\, cos^2\left(\frac{i\pi}{2}\right) \quad (16)$$

$$C_i = \rho AL\Omega + \frac{\pi^2 i^2}{L}\rho I_s\Omega + \frac{\pi^2 i^2}{2L}\rho J_{ps}\Omega + 2M_d\Omega\, sin^2\left(\frac{i\pi}{2}\right) + \frac{2\pi^2 i^2}{L^2}\rho_d h I_d\Omega\, cos^2\left(\frac{i\pi}{2}\right) + \frac{\pi^2 i^2}{L^2}\rho_d h J_{pd}\Omega\, cos^2\left(\frac{i\pi}{2}\right) \quad (17)$$

$$K_i = \frac{2\pi^3 i^3}{4L^3}EI_s - \frac{1}{2}\rho AL\Omega^2 - \frac{1}{2L}\rho I_s\Omega^2 - M_d\Omega^2\, sin^2\left(\frac{i\pi}{2}\right) - \frac{\pi^2 i^2}{L^2}\rho_d h I_d\Omega^2\, cos^2\left(\frac{i\pi}{2}\right) \quad (18)$$

$$F_i = F(t)\, sin\left(\frac{i\pi}{2}\right) \quad (19)$$

3.2 Solution for Free Response of the System

For free vibration analysis, substituting $F(t) = 0$, Eqs. (14) and (15) reduce to

$$M_i\ddot{V}_i(t) - C_i\dot{W}_i(t) + K_iV_i(t) = 0 \quad (20)$$

$$M_i\ddot{W}_i(t) + C_i\dot{V}_i(t) + K_iW_i(t) = 0 \quad (21)$$

Substituting

$$V_i(t) = \bar{V}_i\, e^{\lambda_i t} \quad (22)$$

and $$W_i(t) = \bar{W}_i\, e^{\lambda_i t} \quad (23)$$

into Eqs. (20) and (21), we get the characteristics equation of the system as

$$M_i\lambda_i{}^4 + \left(C_i{}^2 + 2K_iM_i\right)\lambda_i{}^2 + k_i{}^2 = 0 \quad (24)$$

Eq. (24) is quadratic on $\lambda_i{}^2$ and its roots are given as

$$(\lambda_i)_1{}^2 = -\frac{1}{2}\left[\left\{\left(\frac{C_i}{M_i}\right)^2 + 2\frac{K_i}{M_i}\right\} - \sqrt{\left(\frac{C_i}{M_i}\right)^4 + 4\left(\frac{C_i}{M_i}\right)^2\frac{K_i}{M_i}}\right] \quad (25)$$

$$(\lambda_i)_2{}^2 = -\frac{1}{2}\left[\left\{\left(\frac{C_i}{M_i}\right)^2 + 2\frac{K_i}{M_i}\right\} + \sqrt{\left(\frac{C_i}{M_i}\right)^4 + 4\left(\frac{C_i}{M_i}\right)^2\frac{K_i}{M_i}}\right] \quad (26)$$

Then, the natural frequencies corresponding to backward whirl and forward whirl are respectively given by

$$(\lambda_i)_1 = \sqrt{\frac{1}{2}\left[\left\{\left(\frac{C_i}{M_i}\right)^2 + 2\frac{K_i}{M_i}\right\} - \sqrt{\left(\frac{C_i}{M_i}\right)^4 + 4\left(\frac{C_i}{M_i}\right)^2\frac{K_i}{M_i}}\right]} \quad (27)$$

$$(\lambda_i)_2 = \sqrt{\frac{1}{2}\left[\left\{\left(\frac{C_i}{M_i}\right)^2 + 2\frac{K_i}{M_i}\right\} + \sqrt{\left(\frac{C_i}{M_i}\right)^4 + 4\left(\frac{C_i}{M_i}\right)^2\frac{K_i}{M_i}}\right]} \quad (28)$$

3.3 Determination of Force due to Water Jet

During the one complete rotation of the Pelton wheel, the jet does not strike the buckets for certain interval as there is gap between two buckets. Hence force exerted by the water jet on the disk can be approximated by the series of pulses as shown in Fig. 2, where $t_2 - t_1$ ($= t_4 - t_3 = t_6 - t_5 = ..$) is the duration of each pulse which is proportional to the bucket thickness to the circumference of the equivalent runner wheel and T is the period of one revolution of the runner wheel.

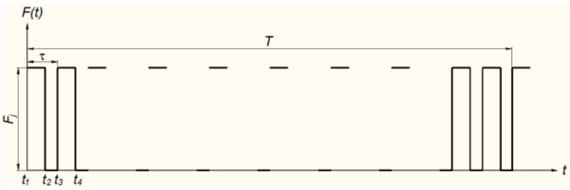

Fig. 2. Pulses of force due to water jet on Pelton turbine.

The force due to water jet can be defined for a period τ mathematically as

$$F(t) = \begin{cases} F_j & t_1 \le t \le t_2 \\ 0 & t_2 < t < t_3 \end{cases} \tag{29}$$

Parameters required for calculation of jet force F_j are taken from [34].

Since the force exerted by the water jet is periodic but non-harmonic, it is converted into harmonic terms by using Fourier series expansion as

$$F(t) = a_0 + \sum_{n=1}^{\infty}\left[a_n \cos\left(\frac{2n\pi}{\tau}t\right) + b_n \sin\left(\frac{2n\pi}{\tau}t\right)\right] \tag{30}$$

where

$$a_0 = \frac{1}{\tau}\int_0^{\tau} F(t)dt \tag{31}$$

$$a_n = \frac{2}{\tau}\int_0^{\tau} F(t)\cos\left(\frac{2n\pi}{\tau}t\right)dt \tag{32}$$

$$b_n = \frac{2}{\tau}\int_0^{\tau} F(t)\sin\left(\frac{2n\pi}{\tau}t\right)dt \tag{33}$$

3.4 Solution for Forced Response of the System

Using Eqs. (14) and (15) with Eq. (30), the forced vibration equation for i^{th} mode (where i is odd) of the system can be rewritten as

$$M_i\ddot{V}_i(t) - C_i\dot{W}_i(t) + K_iV_i(t) = a_0 + \sum_{n=1}^{\infty}\left[a_n \cos\left(\frac{2n\pi}{\tau}t\right) + b_n \sin\left(\frac{2n\pi}{\tau}t\right)\right] \tag{34}$$

$$M_i\ddot{W}_i(t) + C_i\dot{V}_i(t) + K_iW_i(t) = 0 \tag{35}$$

Assuming steady state response of i^{th} mode of the system due to n^{th} harmonics of force due to water jet as

$$[V_{ir}(t)]_n = \bar{V}_{0i} + (\bar{V}_{ci})_n \cos\left(\frac{2n\pi}{\tau}t\right) + (\bar{V}_{si})_n \sin\left(\frac{2n\pi}{\tau}t\right) \tag{36}$$

and

$$[W_{ir}(t)]_n = \bar{W}_{0i} + (\bar{W}_{ci})_n \cos\left(\frac{2n\pi}{\tau}t\right) + (\bar{W}_{si})_n \sin\left(\frac{2n\pi}{\tau}t\right) \tag{37}$$

Substituting Eqs. (36) and (37), into Eqs. (34) and (35), we get the expression for $(\bar{V}_{0i})_n$, $(\bar{V}_{ci})_n$, $(\bar{V}_{si})_n$, $(\bar{W}_{0i})_n$, $(\bar{W}_{ci})_n$ and $(\bar{W}_{si})_n$ required for the steady state response of i^{th} mode of the system due to n^{th} harmonics of force as

$$\bar{V}_{0i} = \frac{a_0}{K_i} \tag{38}$$

$$(\bar{V}_{ci})_n = \frac{a_n(K_i\tau^2 - 4M_i\pi^2n^2)\tau^2}{16{M_i}^2\pi^4n^4 - 4({C_i}^2 + 2K_iM_i)\pi^2n^2\tau^2 + {K_i}^2\tau^4} \tag{39}$$

$$(\bar{V}_{si})_n = \frac{b_n(K_i\tau^2 - 4M_i\pi^2n^2)\tau^2}{16M_i^2\pi^4n^4 - 4\left(C_i^2 + 2K_iM_i\right)\pi^2n^2\tau^2 + K_i^2\tau^4} \quad (40)$$

$$\bar{W}_{0i} = 0 \quad (41)$$

$$(\bar{W}_{ci})_n = -\frac{2b_nC_i\pi n\tau^3}{16M_i^2\pi^4n^4 - 4\left(C_i^2 + 2K_iM_i\right)\pi^2n^2\tau^2 + K_i^2\tau^4} \quad (42)$$

$$(\bar{W}_{si})_n = \frac{2a_nC_i\pi n\tau^3}{16M_i^2\pi^4n^4 - 4\left(C_i^2 + 2K_iM_i\right)\pi^2n^2\tau^2 + K_i^2\tau^4} \quad (43)$$

Then the steady state response of i^{th} mode of the system due to all harmonics of force can be determined as

$$V_{ir}(t) = \bar{V}_{0i} + \sum_{n=1}^{\infty}\left[(\bar{V}_{ci})_n\, cos\left(\frac{2n\pi}{\tau}t\right) + (\bar{V}_{si})_n\, sin\left(\frac{2n\pi}{\tau}t\right)\right] \quad (44)$$

and

$$W_{ir}(t) = \sum_{n=1}^{\infty}\left[(\bar{W}_{ci})_n\, cos\left(\frac{2n\pi}{\tau}t\right) + (\bar{W}_{si})_n\, sin\left(\frac{2n\pi}{\tau}t\right)\right] \quad (45)$$

Then general forced response of the system due to all modes (i = 1, 2, 3,……m) is given by

$$v_r(x,t) = \sum_{i=1}^{m}\left[\left\{\bar{V}_{0i} + \sum_{n=1}^{\infty}\left[(\bar{V}_{ci})_n\, cos\left(\frac{2n\pi}{\tau}t\right) + (\bar{V}_{si})_n\, sin\left(\frac{2n\pi}{\tau}t\right)\right]\right\} sin\left(\frac{i\pi x}{L}\right)\right] \quad (46)$$

and

$$w_r(x,t) = \sum_{i=1}^{m}\left[\left\{\sum_{n=1}^{\infty}\left[(\bar{W}_{ci})_n\, cos\left(\frac{2n\pi}{\tau}t\right) + (\bar{W}_{si})_n\, sin\left(\frac{2n\pi}{\tau}t\right)\right]\right\} sin\left(\frac{i\pi x}{L}\right)\right] \quad (47)$$

4. Numerical Results and Discussion

To have interpretation of the analytical expressions obtained for free and forced responses of the system, the values of system parameters are taken as listed in Table 1.

Table 1. Parameters of the system

Parameters	**Value**
Density of shaft material, ρ	7860 kg/m^3
Cross-sectional area of the shaft, A	0.8042 × 10^{-3} m^2
Length of the shaft, L	0.52 m
Modulus of Elasticity of shaft material, E	202 × 10^9 GPa
Area moment of inertia of the shaft section, I_s	5.1472 × 10^{-8} m^4
Polar moment of area of the shaft section, J_{ps}	1.0294× 10^{-7} m^4
Density of Runner material, ρ_d	8550 kg/m^3
Mass of Runner wheel, M_d	10.564 kg
Thickness of Runner, h	35 mm
Area moment of inertia of the disk, I_d	0.5527 × 10^{-4} m^4
Polar moment of area of the shaft section, J_{pd}	0.11053 × 10^{-3} m^4

4.1 Critical Speeds (Natural Frequencies) and Campbell Diagram

Using Eqs. (16), (17) and (18), equivalent mass (M_i), equivalent damping coefficient (C_i) and stiffness (K_i) for the first three modes are determined and shown in Table 2.

Table 2. Equivalent parameters for the first three modes

Equivalent Parameters	**First Mode**	**Second Mode**	**Third Mode**
Mass (M_i)	12.2085 kg	4.0798 kg	12.2393 kg
Damping	24.4247	13.0384 Ω	24.5478 Ω

coefficient (C_i)	Ω N.s/m	N.s/m	N.s/m
Stiffness (K_i)	$(3.6223 \times 10^6 - 12.2085\ \Omega^2)$ N.m	$(5.7957 \times 10^7 - 4.0798\ \Omega^2)$ N.m	$(2.9341 \times 10^8 - 12.2393\ \Omega^2)$ N.m

Then, the natural frequencies corresponding to backward whirl and forward whirl can be found by using Eqs. (27) and (28). This can be presented in the form of Campbell diagram as shown in Fig. 3.

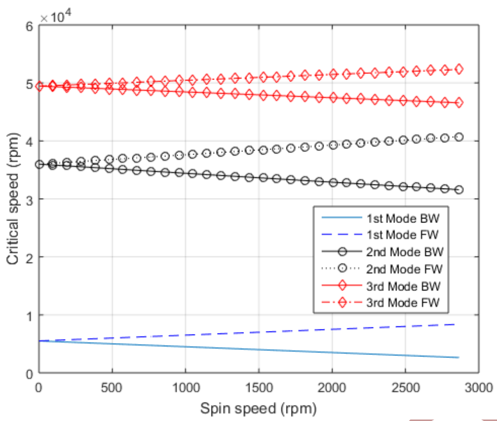

Fig. 3. Campbell diagrams for first three modes

Natural frequencies of each mode corresponding to zero spin speed are the natural frequencies of first three modes of the simply supported beam. As the spin speed increases, critical speed for backward whirl of each mode decreases, whereas, the critical speed for forward whirl for each mode increases. At lower speeds, bending stiffness will have higher value than the stiffness due to centrifugal effect (centrifugal stiffening). During backward whirl, centrifugal stiffening will act opposite to elastic restoring force and, therefore, critical speed for backward whirl decreases with the increase in spin speed as shown in Fig. 3. During forward whirl, centrifugal stiffening will act in the same direction to elastic restoring force and, therefore, critical speed for forward whirl increases with the increase in spin speed as shown in Fig.3.

4.2 Fourier Series Representation of Force due to Water Jet

The values of variables F_j, t_2 and τ for the jet force shown in Fig. 2 are found by [34] as 193 N, 0.00148 s and 0.0025 s respectively. Then coefficients a_0, a_n and b_n for the Fourier series are determined from Eqs. (31), (32) and (33) as

$$a_0 = 228.512\, sin(1.57079k) \qquad (48)$$

$$a_n = \frac{30.7169 sin(1.57079k)}{n} sin(3.71965n) \qquad (49)$$

$$b_n = \frac{30.7169 sin(1.57079k)}{n}[1 - cos(3.71965n)] \qquad (50)$$

Coefficients a_0, a_n and b_n for the first five harmonics are considered by using Eqs. (49) and (50) to determine the forced response of the system. Considering up to fifth harmonics, the approximated force exerted by the water jet on the runner wheel for one-sixteenth revolution of the runner will be as shown in Fig. 4.

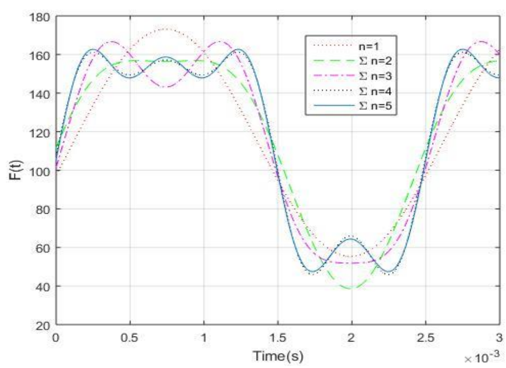

Fig. 4. Fourier series representation (up to first five harmonics $n = 5$) of the force exerted by the water jet

Addition of higher order harmonics increases ripples at the peak but does not affect the peak amplitude value significantly. Hence, harmonics up to the order of five are considered for further analysis.

4.3 Forced Response of the System

Then by using Eqs. (46) and (47), the steady state response for the transverse vibration of the system considering up to third mode are determined and presented in the graphical form.

Substituting $x = L/4$, into the expressions obtained from Eqs. (46) and (47), we can get the steady state response for the transverse vibration of the shaft at its quarter length, and it can be presented in the form response plots as shown in Fig. 5 and Fig. 6.

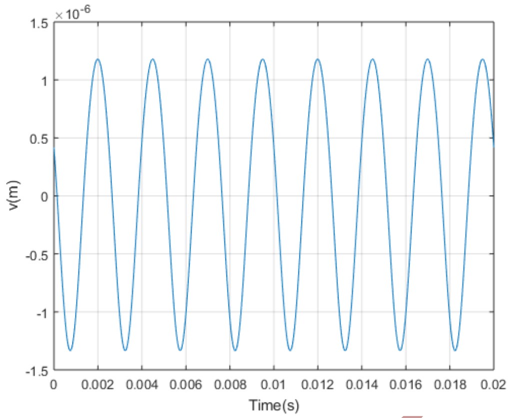

Fig. 5. Transverse displacement of shaft at $x = L/4$ in horizontal direction for $\Omega = 1500$ rpm

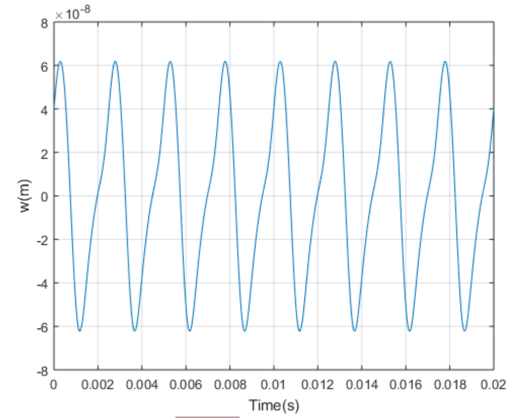

Fig. 6. Transverse displacement of shaft at $x = L/4$ in vertical direction for $\Omega = 1500$ rpm

Similarly, substituting $x = L/2$, into the expressions obtained from Eqs. (46) and (47), we can get the steady state response for the transverse vibration of the disk, and it can presented in the form response plots as shown in Fig. 7 and Fig. 8.

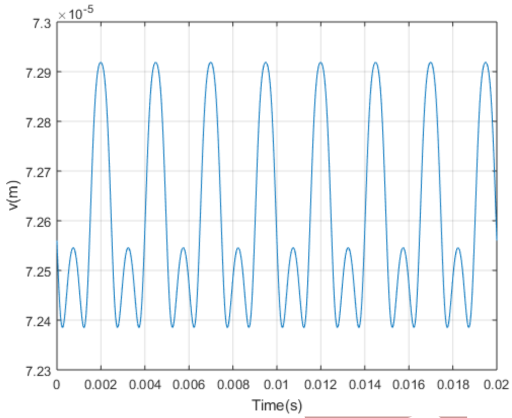

Fig. 7. Transverse displacement of disk in horizontal direction for $\Omega = 1500$ rpm

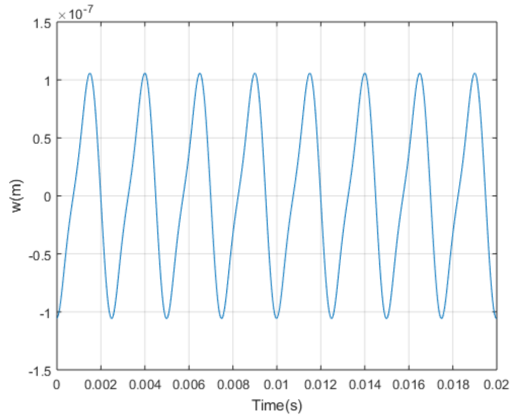

Fig. 8. Transverse displacement of disk in vertical direction for $\Omega = 1500$ rpm

Form Figs. 5 to 8 it is found that the vibration amplitudes in y direction is significantly higher than that in the z direction. Higher vibration amplitude in y direction is due to the impact of jet. The vibration response in z direction is almost sinusoidal throughout the length of the shaft. The vibration response in y direction is almost sinusoidal in the region far from the disk and it has a distorted form in the region near the midspan of the shaft or disk location.

5. Conclusions

In this paper, dynamic behaviour of the Pelton turbine is studied by modelling it as a rigid disk attached on an Euler-Bernoulli shaft. The governing equation of the system for bending vibrations in two transverse directions are found to be coupled system of differential equations. Performing free vibration analysis, the critical speeds of the system for an operating speed of Ω = 1500 rpm for the first three modes are found to be 4001 rpm, 33644 rpm and 47944 rpm for the backward whirl and 7003 rpm, 38437 rpm and 50953 rpm for the forward whirl respectively.

For the forced vibration analysis, the force provided by the water jet is approximated as Fourier series up to the fifth harmonic components. Then, steady state response for bending vibration of the system is determined by applying superposition principle. The peak amplitude of bending vibration at the midspan of the shaft (disk location) in the direction of jet for an operating speed of Ω = 1500 rpm is found to be 73 μm. Similarly, the peak amplitude of bending vibration at the midspan of the shaft (disk location) in the vertical direction for an operating speed of Ω = 1500 rpm is found to be 0.1 μm.

Acknowledgement

We would like to acknowledge the partial support provided by the National Academy for Science and Technology, Nepal for this study.

References

[1] M. Sabuncu and A. Kacar, "Critical Speeds of Continuous Shaft-Disc System," *Vibration and Wear in High Speed Rotating Machinery* , pp. 241-251, 1990.

[2] C. Rajalingham, R. B. Bhat, and G. D. Xistris, "Influence of External Damping on the Stability and Response of a Horizontal Rotor with Anisotropic Bending Stiffness," *Tribology Transactions*, pp. 393-398, 1993.

[3] C. W. Lee and J. S. Yun, "Dynamic Analysis of Flexible Rotors Subjected to Torque and Force," *Journal of Sound and Vibration* , pp. 439-452, 1996.

[4] N. Khader, A. Atoum, and A. Al-Qaisia, "Theoretical and Experimental Modal Analysis of Multiple Flexible Disk-Flexible Shaft System," 2007.

[5] T.A.N. Silva and N.M.M. Maia, "Modelling a Rotating Shaft as an Elastically Restrained Bernoulli-Euler Beam," *Experimental Techniques*, 2011.

[6] C. Chattoraj, S.N. Sengupta, and M. C. Majumder, "Analysis of Dynamic Behaviour a Rotating Shaft with Central Mono-Disk," *International Journal of Engineering & Technology Research*, pp. 77-88, 2013.

[7] O. Gundogdu, K. Alnefaie, and H. Diken, "Modelling and Analysis of a Jeffcott Rotor as a Continuous Cantilever Beam and an Unbalanced Disk System," *Gazi University Journal of Science Part A: Engineering And Innovation*, pp. 77-85, 2014.

[8] M Shahgholi and S.E. Khadem, "Analysis of Stability and Bifurcation of an Asymmetrical Rotor," in *Proceedings of the ASME 2015 Dynamic Systems and Control Conference*, Columbus, Ohio, USA, 2015.

[9] X. Lin, R. Zhou, and N. Xiao, "Influence Characteristics of Shaft and Disk Models on Natural Frequency of Single-Rotor System," *Applied Mechanics and Materials*, pp. 490-494, 2014.

[10] D. J. Han, "Complex Harmonic Modal Analysis of Rotor Systems," *Journal of Mechanical Science and Technology*, pp. 2735-2746, 2015.

[11] D. G. Huang, "Characteristics of Torsional Vibration of a Shaft with Unbalance," *Journal of Sound and Vibration*, pp. 692-698, 2007.

[12] C. O. Chang and J. W. Cheng, "Non-linear Dynamical and Instability of a Rotating Shaft-Disk System," *Journal of Sound and Vibration* , pp. 433-454, 1993.

[13] G. Genta and C. Delprete, "Acceleration Through Critical Speeds of an Anisotropic, Non-Linear Torsionally Stiff Rotor with Many Degrees of Freedom," *Journal of Sound and Vibration* , pp. 369-386, 1995.

[14] T. Inoue and Y. Ishida, "Chaotic Vibration and Internal Resonance Phenomena in Rotor Systems," *Journal of Vibration and Acoustics, Transactions of the ASME*, pp. 156-169, 2006. http://vibrationacoustics.asmedigitalcollection.asme.org/article.aspx?articleid=1470832

[15] H. Diken and I. G. Tadjbakhsh, "Non-Linear Vibration Analysis and Subharmonic Whirl Frequencies of the Jeffcott Rotor Model," *Journal of Sound and Vibration*, pp. 117-125, 2001. https://www.sciencedirect.com/science/article/pii/S0022460X00933947

[16] M. R. Shad, G. Michon, and A Berlioz, "Modelling and analysis of nonlinear rotordynamics due to higher order deformations in bending," *Applied Mathematical Modelling*, pp. 2145-2159, 2011.

[17] H. P. Phadatare and B. Pratiher, "Nonlinear Frequencies and Unbalanced Response Analysis of High Speed Rotor-Bearing Systems," *Procedia Engineering*, pp. 801-809, 2016.

[18] B. O. Al-Bedoor, "Modelling the coupled torsional and lateral vibrations of unbalanced rotors," *Comput. Methods Appl. Mech. Engrg.*, pp. 5999-6008, 2001.

[19] L. Xiang and S. Yang, "Analysis of Flexural and Torsional Vibration for Turbogenerator Shafts on Power Impact," *Advanced Materials Research*, pp. 2498-2501, 2010.

[20] K. Alnefaie, "Lateral and Longitudinal Vibration of a Rotating Flexible Beam Coupled with Torsional Vibration of a Flexible Shaft," *World Academy of Science, Engineering and Technology*, pp. 317-324, 2013.

[21] H. Kojima and K. Nagaya, "Nonlinear Torsional Vibrations of a Rotating Shaft System with a Magnet Couplling," *Bulletin of the JSME*, pp. 1258-1263, 1984.

[22] A. Muszynska and P. Goldman, "Chaotic Responses of Unbalanced Rotor/Bearing/Stator Systems with Looseness or Rubs," *Chaos, Solitons & Fractals*, pp. 1683-1704, 1995.

[23] M. Behzad and M. Asayesh, "Vibration Analysis of Rotating Shaft with Loose Disk," *IJE Transactions B: Applications*, pp. 385-393, 2002.

[24] M. F. A. Azeez and A. F. Vakakis, "Numerical and experimental analysis of a continuous overhung rotor undergoing vibro-impacts," *International Journal of Non-Linear Mechanics*, pp. 415-435, 1999.

[25] X. Shen, J. Jia, and M. Zhao, "Numerical Analysis of a Rub-impact Rotor-bearing System with Mass Unbalance," *Journal of Vibration and Control*, pp. 1819-1834, 2007.

[26] C. W. C. Jian and C. K. Chen, "Chaos of rub–impact rotor supported by bearings with nonlinear suspension," *Tribology International*, pp. 426-439, 2009.

https://www.sciencedirect.com/science/article/pii/S0301679X08001874

[27] H.M. Khanlo, M. Ghayour, and S. Ziaei-Rad, "Chaotic vibration analysis of rotating, flexible, continuous shaft-disk system with a rub-impact between the disk and the stator," *Commun Nonlinear Sci Numer Simulat*, pp. 566-582, 2011.

[28] H.M. Khanlo, M. Ghayour, and S. Ziaei-Rad, "The effects of lateral–torsional coupling on the nonlinear dynamic behaviour of a rotating continuous flexible shaft–disk system with rub–impact," *Commun Nonlinear Sci Numer Simulat*, pp. 1524-1538, 2013.

[29] W. Jiao, Q. Yuan, and Y. Chang, "Study on the coupled bending-torsional vibration of unbalanced rotor system with external excitations," *IEEE International Conference on Computer Science and Automation Engineering (CSAE)*, 2012.

[30] H. Ma, X. Y. Tai, H. L. Yi, S. Lv, and B. C. Wen, "Nonlinear dynamic characteristics of a flexible rotor system with local rub-impact," *Journal of Physics: Conference Series*, 2013.

[31] X. Tai, H. Ma, F. Liu, Y. Liu, and B. Wen, "Stability and steady-state response analysis of a single rub-impact rotor system," *Arch Appl Mech*, pp. 133-148, 2013.

[32] A. M. Wahab, Z. A. Rasid, and A. Abu, "Parametric Instability of Static Shafts-Disk System Using Finite Element Method," in *5th Asia Conference on Mechanical and Materials Engineering (ACMME 2017)*, 2017.

[33] L. Chen, J. Wang, Q. Han, and F. Chu, "Nonlinear dynamic modelling of a simple flexible rotor system subjected to time-variable base motions," *Journal of Sound and Vibration*, vol. 404, pp. 58-83, 2017.

[34] S Karki, M C Luintel, and L Poudel, "Dynamic Response of Pelton Turbine Unit for Forced Vibration," in *IOE Gradauate Conference*, Kathamndu, 2017.